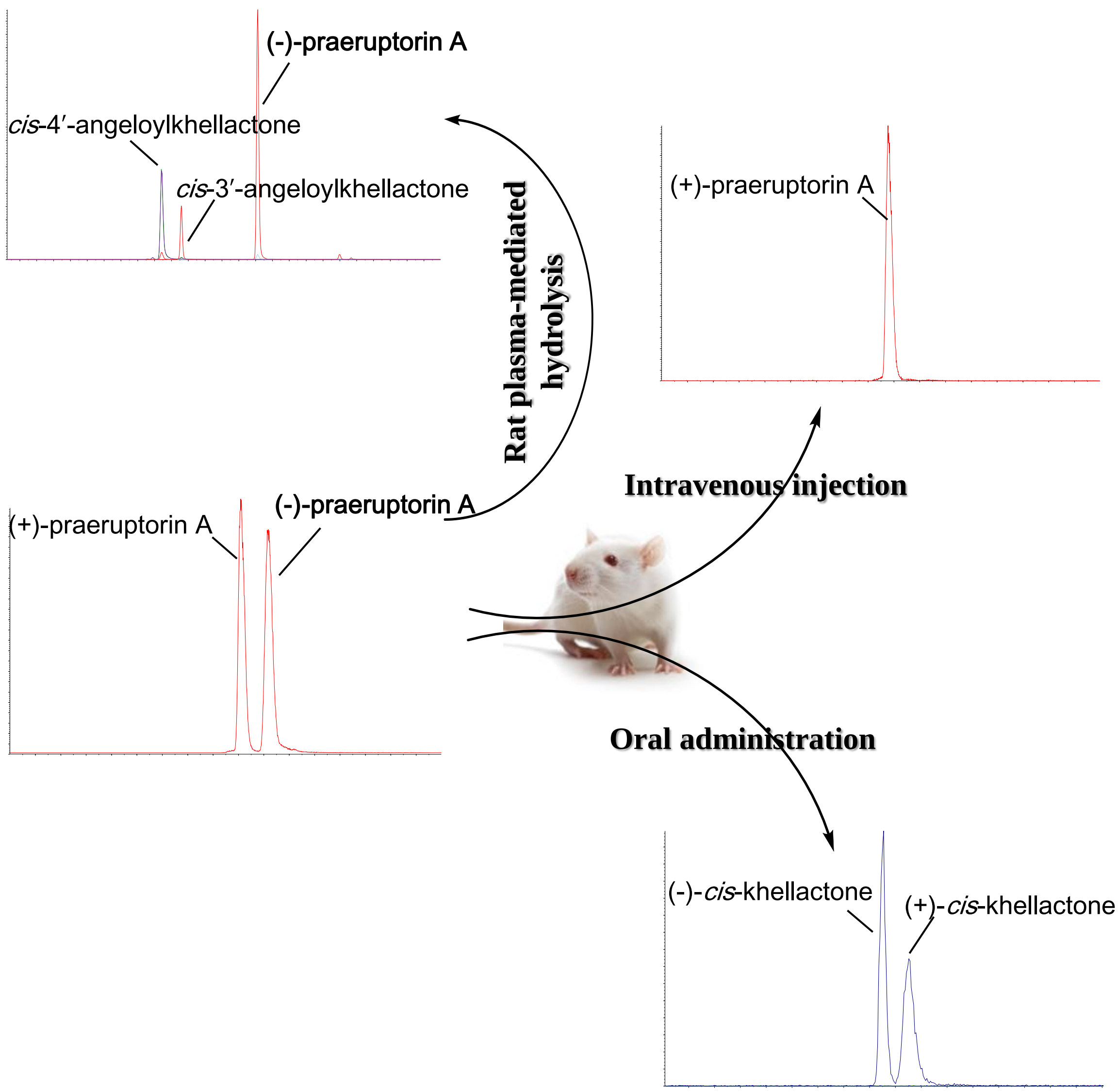
(-)-praeruptorin A
cis-4′-angeloylkhellactone
cis-3′-angeloylkhellactone
Rat plasma-mediated hydrolysis
(+)-praeruptorin A
(+)-praeruptorin A
(-)-praeruptorin A
Intravenous injection
Oral administration
(-)-cis-khellactone
(+)-cis-khellactone

# Development of the enantiospecific and chemoselective methods for determination of praeruptorin A enantiomers and their metabolites in rat plasma using chiral and achiral LC-MS/MS

Yuelin Song [a,b#], Wanghui Jing [a#], Pengfei Tu [b,c], Yi-Tao Wang [a*]

[a] State Key Laboratory of Quality Research in Chinese Medicine, Institute of Chinese Medical Sciences, University of Macau, Macao SAR, 999078, China;

[b] Modern Research Center for Traditional Chinese Medicine, Beijing University of Chinese Medicine, Beijing, 100029, P. R. China;

[c] State Key Laboratory of Natural and Biomimetic Drugs, School of Pharmaceutical Sciences, Peking University, Beijing, 100191, P.R. China.

*Correspondence author:

Prof. Yi-Tao Wang

State Key Laboratory of Quality Research in Chinese Medicine, Institute of Chinese Medical Sciences, University of Macau, Macao SAR, China

E-mail: ytwang@umac.mo; Tel: +8538397 4691; Fax: +8532884 1358.

[#]: these two authors contributed equally to this paper.

**Abstract**

Enantioselective pharmacokinetics and metabolism were revealed for (±)-praeruptorin A (PA), the major bioactive component in Peucedani Radix. In present study, we deal with the development and validation of two enantioselective methods for enantiospecific determination of PA enantiomers (*d*/*l*PA) and their metabolites, *cis*-khellactone enantiomers (*d*/*l*CK) in intravenously and orally treated rat plasma using chiral LC-MS/MS, as well as an achiral LC-MS/MS for simultaneous quantitation of the two hydrolyzed products (L1/L2) after incubation of *l*PA in fresh rat plasma. AD-RH and Extend-$C_{18}$ columns were employed for enantioselective and chemoselective separation, respectively, while the detection was performed on a hybrid triple quadrupole-linear ion trap mass spectrometer with electrospray ionization inlet using positive selected reaction monitoring mode. The calibration curves of all targeted components showed good linearity (r > 0.992) over respective concentration ranges (*d*PA/*l*PA: 1.00 ~ 4830 ng·mL$^{-1}$; *d*CK/*l*CK: 1.50 ~ 1630 ng·mL$^{-1}$; L1/L2: 1.10 ~ 1080 ng·mL$^{-1}$). Low limits of quantitation for *d*PA/*l*PA, *d*CK/*l*CK and L1/L2 were 1.00/1.00 and 1.50/1.50 ng·mL$^{-1}$ and 1.10/1.10 ng·mL$^{-1}$, respectively. For high, medium and low concentration levels of all analytes, the overall intra- and inter-day variations were less than 9.71%, recoveries ranged 87.7% ~ 113~~.2~~%, and matrix effects were between 91.1% and 109~~.4~~%. Above all, the developed chiral and achiral methods were satisfactory for the determination of *d*PA/*l*PA, *d*CK/*l*CK or L1/L2 in rat plasma.

**Keywords:** *d*/*l*-Praeruptorin A; Enantioselective separation; *d*/*l*-*cis*-Khellactone; Rat plasma; Carboxylesterase; LC-MS/MS

## 1. Introduction

(±)-Praeruptorin A (PA) is widely regarded as the major effective constituent and has been officially documented as the quality control indicator (enantiomerically enriched PA, in fact) for Peucedani Radix (Chinese name: Qian-hu) in Chinese Pharmacopeia [1]. This active natural compound exhibit a wide spectrum of activities on modern pharmacological models, including: acting as a novel calcium channels blocker [2,3] and a potassium channels opener [4], chemopreventive effects [5], anti-inflammation [6,7], suppressing expression of the efflux transporter P-glycoprotein [8] and inhibition of monoamine oxidase [9]. Hence, PA has drawn increasing interests due to its bright prospects in the prevention and therapy of cardiac diseases, as well as cancer treatment.

Usually, one enantiomer is significantly more effective than its antipode, and produces the desired effect despite that enantiomers possess identical physical and chemical properties. In current case, enantiomerically pharmacological properties were mentioned for PA enantiomers (*d*/*l*PA) by many reports. For instance, *d*PA and *l*PA exerted distinct relaxant effects on isolated rat aorta rings [10]; *l*PA exhibited hepatoprotective and NO production inhibitory activities [11], while *d*PA could improve the vascular hypertrophy and inhibit the proliferation of smooth muscle cells [12].

Chiral discriminations can occur at any course of absorption, distribution, metabolism and excretion for enantiomers, such as (+/-)-hyoscyamine, (+/-)-clausenamide, (+/-)-tetrahydropalmatine and (+/-)-securinine [13-16]. As expected, the enantioselective absorption and metabolism between *d*PA and *l*PA, which were mainly induced by carboxylesterase(s)-catalyzed hydrolysis for *l*PA ~~in liver microsomal proteins of rats and humans, in rat plasma and in Caco-2 cells~~, were observed *in vitro* [17,18]. As a consequence, it seems importance to develop enantiospecific methods to clarify the potentially enantioselective pharmacokinetic ~~profiles~~ properties between *d*PA and *l*PA.

Direct chiral liquid chromatography (LC) is widely preferred over gas chromatography [19] for nonvolatile components, since LC can be employed without derivatization [20]. Until now, Chiralpak AD-H and AD-RH columns have been employed to enantioseparate PA enantiomers and *cis*-khellactone enantiomers (*d*/*l*CK) [17,18,21,22]. In current study, Chiralpak AD-RH column was selected to connect with the tandem mass spectrometer due to its reversed-phase feature. An automated system of online solid phase extraction-chiral LC-MS/MS was proposed in our previous study aiming to characterize the enantiospecific pharmacokinetics following oral treatment of Qian-hu extract, and *d*/*l*CK were detected as the major herb-related components [22], which agrees well with the metabolic information of PA and its enantiomers [18,25]. However, enantiospecific pharmacokinetic profiles between *d*PA and *l*PA after *i.v.* and *p.o.* administration of PA or its enantiomers hasn't been addressed, as well as the elucidation for the rapid hydrolysis of *l*PA into (3′*R*, 4′*R*)-4′-angeloylkhellactone (L1) and (3′*R*, 4′*R*)-3′-angeloylkhellactone (L2) by rat plasma carboxylesterase(s) [20]. Therefore, in the present study, we deal with the development and validation of the two chiral methods for simultaneous determination of *d*/*l*PA and their hydrolyzed metabolites, *d*/*l*CK, after *i.v.* and *p.o.* dosing using chiral LC-MS/MS, respectively. In addition, an achiral LC-MS/MS for simultaneous quantitation of L1 and L2 was also developed to account for the quick disappearance of *l*PA after *i.v.* treatment.

## 2. Materials and methods

### 2.1. Chemical Materials

PA was prepared in our lab from Peucedani Radix [18]. *d*PA, *l*PA, *d*CK and *l*CK were obtained by enantiomeric separation of PA and CK using semi-preparative Chiralpak AD-RH column (10 mm × 250 mm I.D., particle size 5 μm, Daicel, Tokyo, Japan) [18,21], respectively. L1 and L2, the two hydrolyzed products of *l*PA in rat plasma were also purified by incubation of *l*PA in fresh rat plasma in our laboratory previously [18]. All the chemical structures (Fig.1) and purities (greater than 98% for all) were determined on the basis of NMR and LC-MS/MS data.7-Ethoxycoumarin (7-EC, purity > 98%) that was adopted as internal standard (IS) for both chiral and achiral LC-MS/MS analysis, as well as bis-nitrophenylphospate (BNPP, a selective inhibitor of carboxylesterase), ~~were~~ was purchased from Sigma-Aldrich Chimie SARL (St. Louis, Mo, USA).

HPLC grade formic acid, dimethylsulfoxide (DMSO), methanol (MeOH) and ACN were purchased from Merck (Darmstadt, Germany). Ultra-pure water was obtained in-house from a Milli-Q plus water purification system (Millipore, Bedford, MA, USA). Both ethyl acetate and *n*-propanediol were of analytical grade and obtained commercially.

### 2.2. Chiral and achiral LC-MS/MS

#### *2.2.1. Chiral LC domain*

The concentrations of *d*/*l*PA and *d*/*l*CK in plasma were enantiomerically determined by chiral LC-MS/MS. The analyte separation was achieved on an Agilent series 1200SL LC system (Agilent Technologies, Santa Clara, CA, USA), comprising of a vacuum degasser (G1379B), a binary pump (G1312B), an auto-sampler with the injection loop at 40 μL (G1367C), and being equipped with a Chiralpak AD-RH column (150 mm × 4.6 mm I.D., particle size 5.0 μm, Daicel), which was maintained at 40$^{o}$C during measurement. The sample manager temperature was set at 4$^{o}$C. The mobile phase consisted of 0.1% HCOOH-$H_2O$ (A) and 0.1% HCOOH-ACN (B) and obliquely delivered for plasma samples following *i.v.* administration and *d*PA/*l*PA standards as follows: 0 ~ 12 min, 50% ~ 90%B, 0.50 ~ 0.65 mL·min$^{-1}$; 12 ~ 13 min, 90% ~ 50%B, 0.65 mL·min$^{-1}$; 13 ~ 16 min, 50%B, 0.65 mL·min$^{-1}$; 16 ~ 17 min, 50%B, 0.65 ~ 0.50 mL·min$^{-1}$; 17 min in total, while the 19-min gradient program for oral administration samples and *d*CK/*l*CK standards was set as: 0 ~ 11 min, 30 ~ 50% B; 11 ~ 13 min, 50 ~ 90% B; 13 ~ 15 min, 90% B; 15 ~ 16 min, 90 ~ 30% B; 16 ~ 19 min, 30% B, and flow rate at 0.65 mL·min$^{-1}$.

#### *2.2.2. Achiral LC domain*

In order to account for the rapid disappearance and to clarify the enzymatic kinetics of *l*PA in rat plasma, an achiral LC-MS/MS-based method was also developed. The same LC system as above and an Agilent Extend-$C_{18}$ column (100 mm × 2.1 mm I.D., particle size 3.5 μm, Agilent) were employed. The column temperature was maintained at 40$^{o}$C, and the sample manager temperature for all *in vitro* samples was set at 4°C. The analytes were eluted using a mobile phase containing A (0.1% HCOOH-$H_2O$) and B (0.1% HCOOH-ACN) with the following 26-min program: 0 ~ 20 min, 30 ~ 60%B, 0.30 mL·min$^{-1}$; 20 ~ 21 min, 60 ~ 30%B, 0.30 ~ 0.45 mL·min$^{-1}$; 21 ~ 25 min 30%B, 0.45 mL·min$^{-1}$; 25 ~ 26 min, 30%B, 0.45 ~ 0.30 mL·min$^{-1}$.

*2.2.3. Optimized Parameters of Mass Spectrometry*

An Api-4000® hybrid triple quadrupole-linear ion trap mass spectrometer (Q-trap, ABSciex, Foster City, CA, USA) equipped with a Turbo V™ ion source served as the detector for both chiral and achiral LC, whose Q3 cell can perform as linear ion trap (LIT) mass unit. Electrospray ionization (ESI) ion optics was tuned using standard polypropylene glycol dilution solvent. Nitrogen was used as the nebulizer, heater, curtain and collision gas. Optimum ion source parameters for analytes were as follows: nebulizer, heater and curtain gas flow rates, 45, 45, 10 units, respectively; ion spray needle voltage, 5000 V; heater gas temperature, 550°C. The selected reaction monitoring (SRM) mode under positive ionization was responsible for all targeted components. Analyst software package version 1.5 (ABSciex) was used to control the whole system and also for data acquisition and processing. The optimized precursor-to-product ion transitions for all analytes were summarized in Table 1, and the values of declustering potential (DP) and collision energy (CE) were also included.

Aiming to detect, identify and semi-quantify the metabolites following oral administration, the ion transitions for potential metabolites (Table 1), mainly generated by step-wise hydrolysis, oxidation and intra-molecular migration, based on our previous study of biotransformation of *d*PA and *l*PA in rat liver microsomes [18] and *in vitro* and *in vivo* metabolism of PA [25] were adopted as predictive precursor-product ion transitions during chiral LC-MS/MS analysis performed for orally treated samples. Furthermore, MS/MS spectra of the metabolites were obtained using enhanced product ion (EPI) function which was triggered by the SRM survey experiment according to an information dependent acquiring (IDA) procedure. When the ion transitions exceeded 500 cps, the relevant precursor ions would be trapped in the Q3 cell to generate whole MS/MS spectra. In addition, the metabolic samples mentioned in our previous studies [18,25] were introduced to identify the metabolites by comparing with the *i.v.* and *p.o.* treated samples under identical LC-MS/MS conditions that adopted in previous reports [18,25].

2.3 Validation of chiral and achiral methods

*2.3.1. Preparation of calibration standards and quality control samples*

DMSO stock solutions of *d*PA, *l*PA, *d*CK, *l*CK, L1 and L2 were mixed within enantiomers (*d*PA *vs.* *l*PA, *d*CK *vs.* *l*CK) or regio-isomers (L1 *vs.* L2), and diluted to the desired concentrations with DMSO. An aliquot of *d*/*l*PA diluted solution was spiked into pooled drug-free male Sprague-Dawley (SD) rat plasma, which contained 2.00 μL BNPP solution (final content: 500 μmol·L$^{-1}$), to afford concentration levels of *d*PA/*l*PA ranging from 1.00 to 4830 ng·mL$^{-1}$ (10 concentration levels in total) for the *i.v.* pharmacokinetic study. The drug-spiked plasma was then mixed with a 2.00 μL aliquot of IS solution (0.100 mmol·L$^{-1}$ in DMSO), and extracted using two volumes of ethyl acetate for two times (2 × 200 μL). After vortex-mixing and centrifugation, both supernatants were carefully transferred into another tube, thoroughly mixed and dried with gentle stream of nitrogen gas in 40$^{o}$C water bath. Following that, the residues were reconstituted using 100 μL 50% aqueous ACN followed by vortex-mixing for 3 min as well as ultrasonic water bath for 10 min. Finally, the obtained solution was filtered through 0.22 μm membrane and a 20.0 μL aliquot of the filtrate was injected into the 17-min chiral LC-MS/MS system. Meanwhile, the calibration samples of *d*CK/*l*CK levels were also prepared following the protocol above to yield the concentration range from 1.50 to 1630 ng·mL$^{-1}$ (10 concentration levels in total), and then these obtained samples were subjected for 19-min chiral LC-MS/MS analysis. Each calibration level was prepared in triplicate.

At the meanwhile, an aliquot (2.00 μL) of L1&L2 mixture was spiked with 198 μL potassium phosphate buffer (~~0.~~100 mmol·L$^{-1}$, pH 7.4) containing denatured plasmic protein (final content: 1.00 mg·mL$^{-1}$) to generate concentration levels of L1/L2 ranging from 1.10 to 1080 ng·mL$^{-1}$ (10 concentration levels in total) for the enzyme kinetic study. Each resultant sample was mixed with equal volume of ice-cold ACN and 2.00 μL aliquot of IS solution (0.100 mmol·L$^{-1}$ in DMSO), and then mixed thoroughly. Precipitated proteins were removed by 15000×*g* centrifugation. Subsequently, the supernatant fluid was filtered and 10.0 μL of the filtrate was injected into the 26-min achiral LC-MS/MS system for analysis. Each calibration level was conducted in triplicate.

Three concentration levels of *d*/*l*PA, *d*/*l*CK, or L1/L2 at high, medium and low levels (Table 2) of their respective calibration curves were chosen as quality control (QC) samples.

*2.3.2. Selectivity and specificity*

The potential chromatographic interference from endogenous substances at the retention windows of the analytes and IS was checked with selectivity assay, while specificity test was performed by comparing chromatographic profile from plasma and incubated samples with the authentic standards using the retention times and MS/MS spectra yielded by the EPI function.

*2.3.3. Linearity*

Each standard curve was fitted using least squares linear regression method *via* plotting the peak area ratios of each analyte to IS *vs.* the theoretical plasma concentration levels in order to obtain acceptable deviations for all of the concentration levels. The acceptance criterions were a correlation coefficient (r) of 0.990 or better for each calibration curve and a back-calculated standard concentration within a 15.0% deviation from the nominal value except at the limit of quantification (20.0% deviation).

*2.3.4. Accuracy and precision*

Accuracy was evaluated by measuring three consecutive batches containing calibration curve standards and was acceptable at the case of RE [(observed concentration/nominal concentration) × 100%] within 85.0% ~ 115%. Meanwhile, intra- and inter-day precision was determined by analyzing each QC sample for six replicates and the relative standard deviations (RSDs, %) were expected to be within ±15% to be tolerant for precision.

*2.3.5. Lower limits of quantification*

The lower limits of quantification (LLOQ), defined as the lowest concentration in the standard curve (r > 0.990) at which RSD was within 20.0% and accuracy was within 100 ± 20.0% by analyzing samples prepared in quintuplicate.

*2.3.6. Stability*

The stock solution stability at refrigerated condition (4°C) was performed by comparing the area response of the analyte (stability samples) with the response of the sample prepared from fresh stock solution and all *d*PA, *l*PA, *d*CK, *l*CK, L1 and L2 could keep intact in DMSO within two months when they were stored at 4°C.

On the other side, short-term stabilities, three cycles of freeze-thaw and long-term stability assays were carried out using high, medium and low concentration levels of QC samples. Short-term stability was assayed by keeping the QC samples at room temperature for 4 h prior to measurement, while long-term stability was evaluated by maintaining QC samples at -20°C for two weeks ahead of thawing and extraction. Freeze-thaw cycle stability assay was performed *via* repeatedly freezing (store at -20°C for 24 hours) and thawing (completely thaw at room temperature) QC samples for three cycles before analysis.

*2.3.7. Extraction efficiency and matrix effect assays*

The extraction recoveries of each analyte (*d*PA, *l*PA, *d*CK or *l*CK) in plasma samples at the three QC levels were determined by comparing peak area ratio obtained from spiked plasma sample with those found by direct injection of a standard solution spiked with blank matrix in 50% aqueous ACN of the same concentration level. The matrix effect of plasma sample was determined by comparing peak area ratio obtained from a standard solution spiked with blank matrix in 50% aqueous

ACN with that obtained by direct injection of a standard solution spiked with 50% aqueous ACN.

Meanwhile, the matrix effect for incubation samples was also investigated. The peak area ratio of each analyte in QC sample was compared with the corresponding peak area ratio obtained by direct injection of the standard in 50% aqueous ACN.

2.4. Preparation of biological samples

*2.4.1. Preparation of PA-treated plasma samples*

Male SD rats (220 ± 15 g) were purchased from Beijing Laboratory Animal Research Center (Beijing, China) and acclimated in laboratory for one week before the experiments. All the studies on animals were in accordance with the Guidelines for the Care and Use of Laboratory Animals in University of Macau, Macao, China. Animals were raised at a temperature of 23 ± 1°C with a 12-h light/dark cycle and relative humidity of 50%. Standard chow and Milli-Q water were provided *ad libitum*. Rats were divided randomly into six groups (*n* = 4 per group for *i.v.* dosing, groups A-C; *n* = 6 per group for *p.o.* administration, groups D-F). A day ahead of administration, a jugular vein cannula (polyethylene, o.d. 0.8 mm, i.d. 0.4 mm) was implanted under light anesthesia with diethyl ether for receiving *i.v.* dosing and blood sampling [24]. After surgery, all rats were permitted to recover and fasted overnight with free access to water. For *i.v.* administration, a single dose of PA (4.00 mg·kg$^{-1}$), *d*PA (2 mg·kg$^{-1}$) or *l*PA (2.00 mg·kg$^{-1}$), which was dissolved in *n*-propanediol : 0.9% NaCl-injectable solution (1:1, *v*/*v*), was injected *via* the catheter to individual groups of rats (groups A-C), and then the cannula was washed by ~~0.~~300 µ~~m~~L of saline containing 40 IU heparin·mL$^{-1}$. On the other side, a single dose of PA (40.0 mg·kg$^{-1}$), *d*PA (20.0 mg·kg$^{-1}$) or *l*PA (20.0 mg·kg$^{-1}$) in normal saline containing 50% *n*-propanediol was orally treated to individual group of rats (groups D-F). Then 0.25 mL of blood samples were collected through the cannula into pre-heparinized Eppendorf tubes at appropriate time intervals as over 18-h (*i.v.*) and 48-h (*p.o.*) periods. After each collection, ~~0.~~250 µ~~m~~L of saline containing 40.0 IU of heparin·mL$^{-1}$ was used to flush the cannula immediately to compensate for blood loss and prevent clotting after each blood sampling. Each blood sample was immediately centrifuged at approximately 3000×*g*, 4°C for 10 min, and then plasma samples were harvested. After that, the plasma samples were processed with the protocols described above.

*2.4.2. Preparation of in vitro incubation samples of lPA*

Pooled blank blood was taken from five drug-free male SD rats (220 ± 15 g) using heparinized syringes, centrifuged at 3000×*g* for 10 min at 4°C to afford the pool of plasma. Fresh rat plasma, the total protein content (35.2 mg·L$^{-1}$) of which was determined using the Lowry's method [26], was used immediately for *in vitro* metabolic experiment. *l*PA (~~0.005~~ 1.93 ~ ~~30~~11580 ~~μ~~ ng~~mol~~·mL$^{-1}$) was incubated with plasma (final content concentration: 1.00 mg·mL$^{-1}$) in potassium phosphate buffer solution (pH 7.4, 100 mmol·L$^{-1}$) for 20 min at the final incubation volume as 200 μL. There were two types of control samples: one contained the denatured plasma protein and the other had no substrate. Subsequently, the incubates were treated using the method mentioned above.

**3. Results**

3.1. Optimization of LC-MS/MS conditions

Positive ESI mode was selected by infusing each analyte and IS into the mobile phase using a T-piece mounted on the Turbo V™ ion source of the mass spectrometer. Precursor ion yield definitely increased with the growth of the ion-spray voltages, and 5500 V was thus selected. The typical values for the LC effluent were adopted for ion source gas flows and ion source temperature. The sodium adduct ions (*m/z* 409 $[M+Na]^+$ for *d*/*l*PA, *m/z* 367 $[M+Na]^+$ for L1/L2) were afforded predominantly as precursor ions for all targeted compounds, except that the protonated ions (*m/z* 263 $[M+H]^+$) were observed as the most abundant for CK enantiomers. Following the confirmation of precursor ions, more than two product ions should be selected when using MS/MS analysis in accordance with relevant legislation [27]. As reported [18], the successive neutral loss of $CH_3COOH$ and $C_4H_7COOH$ moieties were observed as the predominant cleavages for PA enantiomers, while the cleavage of a $C_4H_7COOH$ group was solely detected as characteristic loss for L1/L2 due to the absence of acyl substituent. On the other side, fragment ions at *m/z* 245 and 203 were exhibited as the diagnostic product ion for *d*CK/*l*CK. ~~At last~~Finally, the parameters including DP, CE and CXP were optimized manually. At the meanwhile, the ion transitions and corresponding parameters for potential metabolites *in vivo* were also included following our previous report [25]. The optimum results are summarized in Table 1.

Chromatographic conditions including column type, mobile phase selection, flow rate and column temperature were carefully evaluated. Chiralpak AD-RH column performed better over other types of chiral columns and also exhibited reversed-phase characteristic, thus adopting for enantiomeric separation, while Agilent Extend-$C_{18}$ column was chosen to offer chemoselective separation for the regio-isomers, L1 *vs.* L2. Methanol and ACN were tried in different ratio with buffers like ammonium acetate, ammonium formate as well as acid additives like formic acid and acetic acid in varying strength. It was observed that 0.1% aqueous formic acid-0.1% HCOOH-ACN as the mobile phase was most appropriate to give best sensitivity, efficiency and peak shape for all analytes. For the time-saving purpose, the flow rate was raised to equilibrate the whole system after the last targeted compound was flushed. The injection to injection intervals for the final methods were fixed as 17 min, 19 min and 26 min for *i.v.* treated samples, *p.o.* treated samples and incubated samples, respectively.

## 3.2. Method Validation

### *3.2.1. Selectivity and specificity*

Retention times ($t_R$) of the six analytes and IS in respective LC conditions were summarized in Table 1. Figs. 2-3 illustrated typical chromatograms for blank plasma, plasma spiked with mixed standards, and plasma obtained 0.5 h after *i.v.* and oral administration of PA or its enantiomers, respectively, while Fig. 4 exhibited representative chromatograms for incubation sample of *l*PA with fresh rat plasma. Each analyte was found to be free from interferences in the retention time window

(Figs. 2-4). Satisfactory enantiomeric and chemoselective separations were achieved for most monitored components using the current achiral and chiral LC-MS/MS systems, suggesting that the developed method exhibited high selectivity and specificity.

*3.2.2. Linearity, accuracy, precision and LLOQs*

All the calibration curves for plasma and incubated samples showed good linearity (all correlation factors higher than 0.992) over the concentration ranges tested (*d*PA/*l*PA: 1.00 ~ 4830 ng·mL$^{-1}$; *d*CK/*l*CK: 1.50 ~ 1630 ng·mL$^{-1}$ and L1/L2: 1.10 ~ 1080 ng·mL$^{-1}$) (Table 2). Accuracy expressed in terms of RE was within 93.4 ~ 112~~.3~~% for all calibration levels of the six analytes except the LLOQs, where the RE values were also between 80.7 ~ 117~~.2~~%. The overall intra- and inter-day variations of all analytes were less than 10.0% (1.42 ~ 9.71%) (Table 3). LLOQs for *d*PA/*l*PA and *d*CK/*l*CK were determined as 1.00/1.00 and 1.50/1.50 ng·mL$^{-1}$ (Table 2), respectively, based on both precision and accuracy not more than 20%, while LLOQs for L1 and L2 were 1.10 ng·mL$^{-1}$ in denatured plasmic protein spiked incubation system (Table 2). All the results met the pertinent guidelines [30], suggesting that the developed methods were precise, accurate and sensitive.

*3.2.3. Stability*

All stock solutions were stable for minimum of ~~2~~ two months. All analytes in rat plasma (*d*PA/*l*PA and *d*CK/*l*CK) or in buffer (L1/L2) at room temperature were stable at least for 4 h (bench top stability), and for minimum of three freeze and thaw cycles (all within the ±10.0% assay variability limitation). Spiked samples, which were stored at -20°C for long term stability experiment, were stable for minimum of ~~14~~ fourteen days.

In addition, the interferences from carryover and re-injection were also assessed and the results indicated that influences of these two assays could be ignored due to their extremely low levels.

*3.2.4. Matrix effects and extraction efficiency*

The overall recovery efficiency for PA and CK enantiomers was lower than 113~~.2~~% yet higher than 87.7% for each concentration level, indicating that ethyl acetate is a feasible and appropriate medium for *d*PA, *l*PA, *d*CK and *l*CK extraction.

The matrix effect of QC samples at low, medium and high concentration levels of *d*PA, *l*PA, *d*CK, *l*CK, L1 and L2 was observed to be within the range of 91.1 ~ 109~~.4~~%, indicating that matrix substances would not significantly affect the performance of chromatography or the ionization of analytes, and thus the matrix effect could be neglected.

3.3. Application of developed chiral and achiral methods

The 17-min method was applied to monitor *d*PA and *l*PA in rat plasma after *i.v.* administration of *d*PA, *l*PA or PA. *d*PA was obviously detected following dose of *d*PA or PA. Neither *l*PA dosing nor PA dosing could afford *l*PA prototype in rat plasma after the first 5 minutes. On the other hand, *l*CK and/or *d*CK were observed as the major PA-related components in rat plasma after oral administration of PA racemate or PA enantiomers using the 19-min method. The pharmacokinetic parameters were described in reference [29].

Based on our previously study, carboxylesterase(s)-catalyzed hydrolysis coupled with acyl migration can be occurred for *l*PA in plasma to generate two hydrolyzed products, L1 and L2 [18]. To determine the kinetic parameters of L1 and L2 generated from *l*PA, *l*PA was incubated with pooled rat plasma and the incubated samples were analyzed using the 26-min achiral LC-MS/MS validated above. Reaction conditions, including incubation interval and protein content, were confirmed to ensure that the transformation of *l*PA and the generation of L1/L2 meet the assumption terms of typical Michaelis-Menten model. Finally, protein content as 1.00 mg·mL$^{-1}$, 20 min incubation duration and ~~10~~ ten concentration levels ranged from 1.93 ~ 11580 ng·mL$^{-1}$~~0.005 ~ 30 μmol·L$^{-1}$~~ were performed as the optimal reaction conditions. The chromatogram of *l*PA hydrolysis by rat~~s'~~ plasma for 15 min was shown in Fig. 4. It is clear that *l*PA can quickly be hydrolyzed by rat plasma to two metabolites. The detailed Michaelis constant ($K_m$) and maximum velocity ($V_{max}$) information were archived in reference [29].

The metabolic characterization of PA and its two enantiomers was well achieved in our prior studies [18,25], and oxidation and hydrolysis as well as intra-molecular acyl migration were observed as the major metabolic pathways. Therefore, in current study, the identification of the metabolites was carried out using the MS/MS spectra afforded by EPI scan in combination with comparing with the *in vitro* incubation samples mentioned in our previous work under the identical LC-MS/MS conditions. Only the two hydrolyzed product of *l*PA, L1 and L2 were obviously observed in the *l*PA-dosed and PA-treated plasma following *i.v.* injection. On the other side, the *di*-hydrolyzed products of PA enantiomers, *d*CK and *l*CK, were detected as the major PA-related components in orally treated plasma. Moreover, a mono-oxidated metabolite (D1, molecular weight: 402 Da, $t_R$: 13.4 min) and a C-4′ hydrolyzed product (D2, molecular weight: 344 Da, $t_R$: 13.8 min) were also detected in *d*PA-treated plasma, while a *mono*-oxidated metabolite (L3, molecular weight: 402 Da, $t_R$: 13.2 min) along with L1 (molecular weight: 344 Da, $t_R$: 14.0 min) and L2 (molecular weight: 344 Da, $t_R$: 14.2 min) were observed in *l*PA-treated plasma (Table 1 & Fig. 3). As expected, all the metabolites were distributed in the PA-treated samples.

As described above, the precursor-product ion pairs for *d*PA, the *mono*-oxidated product of *d*PA (D1) and the *mono*-oxidated product of *l*PA (L3) were included in the 19-min method for oral administration. The peak area ratio-time curves of those monitored components were also achieved after oral administration of PA or its two enantiomers using the chiral LC-SRM method for oral administration samples (Figs. S1-3, supplemental data).

Chiral discriminations between enantiomers were widely observed for the pharmacokinetic profiles of many famous clinical used drugs. However, for many racemic or enantiomerically enriched drugs, their enantiospecific pharmacokinetic properties are still ill-defined owing to the unavailability of chiral analytical methods. In current study, two enantiospecific methods were developed and validated for the quantitative analysis of PA enantiomers and their *di*-hydrolyzed products, respectively.

Hydrolysis enzymes, such as carboxylesterases and cholinesterases, are widely distributed in plasma, suggesting a crucial plasma-mediated metabolism for some ester-type compounds or pro-drugs. In current study, crucial hydrolysis occurred for *l*PA rather than *d*PA, despite that the both are *di*-esterified products of *cis*-khellactone, indicating the enantioselective preference for those enzymes. Hence, it is quite necessary to perform enantiospecific determination for enantiomers and also to pay attention to the metabolic stability of xenobiotics in plasma.

A great body of experimental evidences indicated that PA and *d*PA may yield potential benefits for the treatment and prevention of cardiovascular diseases following *i.v.* or oral administration [30,31]. As the most abundant constituent and the major active component in Peucedani Radix (Chinese name: Qian-hu), pharmacokinetics of PA was usually investigated as the mixture of its dextrorotatory and levorotatory forms [23,24] even though that many studies suggested the distinct pharmacological features for these enantiomers. Unraveling the stereoselective pharmacokinetic profiles of PA enantiomers and characterization of potential interactions between two enantiomers will definitely help understand the underlying mechanism of Qian-hu actions as well as developing new drug(s) from the well-recognized traditional herbal medicine. Owing to the enantiospecific absorption and metabolism of the two enantiomers [17,18], simple chiral LC-MS/MS were developed initially, for the first time, to characterize the enantioselective pharmacokinetic profiles of *d*/*l*PA in rat after intravenous and oral dosing and hence to estimate the extent of chiral discrimination.

**5. Conclusion**

Two sensitive, reliable and enantioselective chiral LC–MS/MS and a sensitive, reliable and chemoselective achiral LC–MS/MS have been developed and validated to characterize the pharmacokinetic profiles of PA and its two enantiomers, *d*CK and *l*CK, and to clarify the extensive hydrolysis of *l*PA in rat plasma. The developed methods were successively applied for the characterization of *i.v.* and oral pharmacokinetic profiles of PA enantiomers, and the results were archived in reference [29].The peak area-time curves of *d*PA prototype, the mono-oxidated product of *d*PA and the mono-oxidated product of *l*PA were also obtained following oral administration of PA and its enantiomers using the developed chiral LC-MS/MS for oral administration. The present study, in combination with our previous reports and the results from Xu *et al.* [10], provides sound scientific evidences to support that the dextrorotatory form of PA (*d*PA) is the eutomer while its antipode (*l*PA) should be regarded as the distomer.

**Acknowledgement**

The authors acknowledge financial support from the National Basic Research Program of China 973 program (Grant No.2009CB522707), the Macao Science and Technology Development Fund (077/2011/A3, 074/2012/A3) and the Research Fund of the University of Macau (MYRG 208 (Y3-L4)-ICMS11-WYT, and MRG012/WYT/2013/ICMS, MRG013/WYT/2013/ICMS).

**Appendix A. Supplementary data**

Supplementary data associated with this article can be found, in the online version, at ...

**References**

1 The State Pharmacopoeia Commission of P.R. China. Radix Peucedani. In: Pharmacopoeia of the People’s Republic of China Beijing, China: Chemical Industry Press; 2010: (Vol I) pp. 248.

2 T. Kozawa, K. Sakai, M. Uchida, T. Okuyama and S. Shibata, *J. Pharm. Pharmacol.*, 1981, **33**, 317–320

3 T.H. Chang, H. Adachi, T. Okuyama and K.Y. Zhang, *Acta Pharmacol. Sin.*, 1994, **15**, 388-391.

4 S.L. Zhang, J.M. Li, Q.H. Xiao, A.H. Wu, Q. Zhao, G.R. Yang and K.Y. Zhang, *Acta Pharmacol. Sin.*, 2001, **22**, 813–816.

5 T.G. Liang, W.Y. Yue and Q.S. Li, *Molecules*, 2010, **15**, 8060-8071.

6 T.H. Chang, X.Y. Liu, X.H. Zhang and H.L. Wang, *Acta Pharmacol. Sin.*, 2002, **23**, 769-774.

7 P.J. Yu, W. Ci, G.F. Wang, J.Y. Zhang, S.Y. Wu, W. Xu, H. Jin, Z.G. Zhu, J.J. Zhang, J.X. Pang and S.G. Wu, *Phytother. Res.*, 2011, **25**, 550-556.

8 X.L. Shen, G.Y. Chen, G.Y. Zhu and W.F. Fong, *Bioorgan. Med. Chem.*, 2006, **14**, 7138-7145.

9 D.T.L. Huong, H.C. Choi, T.C. Rho, H.S. Lee, M.K. Lee and Y.H. Kim, *Arch. Pharm. Res.*, 1999, **22**, 324-326.

10 Z. Xu, X. Wang, Y. Dai, L. Kong, F. Wang, H. Xu, D. Lu, J. Song and Z. Hou, *Chem. Biol. Interact.*, 2010, **186**, 239–246.

11 H. Matsuda, T. Murakami, T. Kageura, K. Ninomiya, I. Toguchida, N. Norihisa and M. Yoshikaca, *Bioorg. Med. Chem. Lett.*, 1998, **8**, 2191-2196.

12 E.H. Wei, M.R. Rao, X.Y. Chen, L.M. Fan and Q. Chen, *Acta Pharmacol. Sin.*, 2002, **23**, 129-132.

13 H. John, J. Mikler, F. Worek and H. Thiermann, *Drug Test Anal.*, 2011, **4**, 194-198.

14 C.J. Zhu and J.T. Zhang, *Chirality*, 2003, **15**, 669-673.

15 Z.Y. Hong, G.R. Fan, Y.F. Chai, X.P. Yin and Y.T. Wu, *Chirality,* 2005, **17**, 293-296.

16 X.H. Li, J.L. Zhang and T.H. Zhou, *YaoXueXueBao*, 2002, **37**, 50-53.

17 W.H. Jing, Y.L. Song, R. Yan, H.C. Bi, P.T. Li and Y.T. Wang, *Xenobiotica*, 2011, **41**, 71-81.

18 Y.L. Song, W.H. Jing, H.Y. Zhao, R. Yan, P.T. Li and Y.T. Wang, *Xenobiotica*, 2012, **42**, 231-247.

19 W. Liu, Z. Chen, H. Xu, Y. Shi and Y. Chen, *J. Chromatogr. A*, 1991, **547**, 509-515.

20 P. Wang, S. Jiang, D. Liu, H. Zhang and Z. Zhou, *J. Agric. Food Chem.*, 2006, **54**, 1577-1583.

21 Y.L. Song, Q.W. Zhang, Y.P. Li, R. Yan and Y.T. Wang, *Molecules*, 2012, **17**, 4236-4251.

22 Y.L. Song, W.H. Jing, F.Q. Yang, Z. Shi, M.C. Yao, R. Yan and Y.T. Wang, *J. Pharm. Biomed. Anal.*, 2014, **88**, 269-277.

23 H. Ruan, Z. Zhang and X. Zhu, *Biomed. Chromatogr.*, 2010, **24**, 1193-1198.

24 Z. Zhang, Y.Y. Liu, M.Q. Su, X.F. Liang, W.F. Wang and X. Zhu, *Phytomedicine*, 2011, **18**, 527-532.

25 Y.L. Song, W.H. Jing, R. Yan and Y.T. Wang, *J. Pharm. Biomed. Anal.*, 2014, **90**, 98-110.

26 O.H. Lowry, N.J. Rosenbrough, A.L. Farr and R.J. Randall, *J. Biol. Chem.*, 1951, **193**, 265–275.

27 The Commission of the European communities, Implementing Council Directive 96/23/EC concerning the performance of analytical methods and the interpretation of results. Brussels, 2002, pp. L221/16–L221/17.

28 U.S. Food and Drug Administration, Bioanalytical method validation, in: 654 Guidance for Industry, U.S. Food and Drug Administration, 2001, pp. 1-25.

29 Y.L. Song, R.N. Zhou, R. Yan and Y.T. Wang, *Drug Metabol, Rev.,* 2011, **43**, S182-183.

30 H. Chang, X.Y. Chu, J. Zou and T.H. Chang, *Chin. Med. J.*, 2007, **120**, 2256-2259.

31 M.R. Rao, W.B. Liu, P.Q. Liu and E.H. Wei, *Zhongguo Yaoxue Zazhi*, 2002, **11**, 110-114.

## Figure Legends

**Figure 1** Chemical structures of (+)-praeruptorin A (*d*PA), (-)-praeruptorin A (*l*PA), (+)-*cis*-khellactone (*d*CK), (-)-*cis*-khellactone (*l*CK), (3′*R*, 4′*R*)-4′-angeloylkhellactone (L1) and (3′*R*, 4′*R*)-3′-angeloylkhellactone (L2).

Formatted: Font: Italic

Formatted: Font: Italic

Formatted: Font: Italic

Formatted: Font: Italic

**Figure 2** Typical LC-SRM chromatograms of blank plasma (A); blank plasma spiked IS (7-EC, B); blank plasma spiked IS and PA (C); plasma after *i.v.* administration of PA (D), *d*PA (E), *l*PA (F) at 0.5 h.

**Figure 3** Representative LC-SRM chromatograms of blank plasma (A); blank plasma spiked IS (7-EC, B); blank plasma spiked IS and PA (C); plasma after oral administration of PA (D), *d*PA (E), *l*PA (F) at 0.5 h.

**Figure 4** Typical LC-SRM chromatograms of *l*PA-free incubate (A); *l*PA-free incubate spiked IS (7-EC, B); blank plasma spiked IS and L1 & L2 (C); incubation of *l*PA with rat plasma at the concentration of ~~5~~ 1930 ng~~μmol~~·mL$^{-1}$ for 0 min (D) and 15 min (E).

Table 1 Precursor-to-product ion transitions and parameters of SRM mode

| | Retention time (min) | Q1/Q3 | Dwell time (ms) | DP (V) | EP (V) | CE (V) | CXP (V) |
|---|---|---|---|---|---|---|---|
| *d*PA | 9.2[a]/16.2[b] | 409.3/227.5 | 150 | 130.0 | 10.0 | 35.6 | 10.0 |
| | | 327.7/227.5[c] | 150 | 77.0 | 10.0 | 22.9 | 17.0 |
| *l*PA | 10.6[a] | 409.3/227.5 | 150 | 130.0 | 10.0 | 35.6 | 10.0 |
| | | 327.7/227.5[c] | 150 | 77.0 | 10.0 | 22.9 | 17.0 |
| *l*CK | 8.5[b] | 263.1/245.1 | 150 | 86.0 | 10.0 | 15.7 | 12.0 |
| | | 263.1/203.1[c] | 150 | 86.0 | 10.0 | 21.0 | 12.0 |
| *d*CK | 9.6[b] | 263.1/245.1 | 150 | 86.0 | 10.0 | 15.7 | 12.0 |
| | | 263.1/203.1[c] | 150 | 86.0 | 10.0 | 21.0 | 12.0 |
| L1 | 14.0[b]/14.1[d] | 367.1/267.1[c] | 150 | 80.0 | 10.0 | 21.1 | 10.0 |
| | | 327.7/227.5 | 150 | 77.0 | 10.0 | 22.9 | 17.0 |
| L2 | 14.2[b]/14.3[d] | 367.1/267.1 | 150 | 80.0 | 10.0 | 21.1 | 10.0 |
| | | 327.7/227.5[c] | 150 | 77.0 | 10.0 | 22.9 | 17.0 |
| D1/L3 | 13.4[b]/13.2[b] | 425.1/245.1[c] | 150 | 130.0 | 10.0 | 36.0 | 12.0 |
| | | 425.1/365.1 | 150 | 130.0 | 10.0 | 26.7 | 12.0 |
| D2 | 13.8 [b] | 367.1/267.1[c] | 150 | 80.0 | 10.0 | 21.1 | 10.0 |
| | | 327.7/227.5 | 150 | 77.0 | 10.0 | 22.9 | 17.0 |
| 7-EC | 9.3[a]/15.7[b] | 191.1//163.5 | 150 | 55.0 | 10.0 | 25.0 | 12.0 |

[a]: the retention time for *i.v.* administration plasma sample; [b]: the retention time for oral administration plasma sample; [c]: the precursor-product ion transition for quantitation; [d]: the retention time for *in vitro* incubation sample in rat plasma.

Table 2 Linear regression data, limits of quantification (LOQ) for all investigated analytes

| Analyte | Linear regression data | | | LOQ ($ng \cdot mL^{-1}$) |
|---|---|---|---|---|
| | Regression equation | r | Test range ($ng \cdot mL^{-1}$) | |
| *d*PA | y = 0.00413 x + 0.00507 | 0.993 | 1.00-4830 | 1.00 |

| | | | | |
|---|---|---|---|---|
| *l*PA | y = 0.00411 x + 0.00436 | 0.992 | 1.00-4830 | 1.00 |
| *d*CK | y = 0.00787 x + 0.00832 | 1.000 | 1.50-1630 | 1.50 |
| *l*CK | y = 0.00778 x + 0.00359 | 1.000 | 1.50-1630 | 1.50 |
| L1 | y = 34.6 x + 0.0452 | 0.995 | 1.10-1080 | 1.10 |
| L2 | y = 16.8 x - 0.00214 | 0.999 | 1.10-1080 | 1.10 |

Table 3 Inter-day and intra-day ($n$= 6) performance parameters of low, medium and high level quality control samples for all analytes

| Analyte | Concentration level | Theoretical concentration ($ng{\cdot}mL^{-1}$) | Measured concentration Intra-day (Mean ± SD) | Intra-day (RSD%) | Measured concentration Inter-day (Mean ± SD) | Inter-day (RSD%) |
|---|---|---|---|---|---|---|
| *d*PA | High | 2420 | 2323 ± 44.1 | 1.~~8~~78 | 2299± 60.0 | 2.40 |
| | Medium | 75.4 | 73.9± 3.99 | 5.40 | 71.6± 5.22 | 7.33 |
| | Low | 2.35 | 2.63 ± 0.213 | 8.13 | 2.68± 0.254 | 9.62 |
| *l*PA | High | 2420 | 2226± 31.2 | 1.~~2~~42 | 2275± 107 | 4.~~3~~28 |
| | Medium | 75.4 | 73.1± 4.90 | 6.72 | 71.6± 4.94 | 6.94 |
| | Low | 2.35 | 2.66± 0.244 | 9.439 | 2.68± 0.265 | 9.71 |
| *d*CK | High | 815 | 774± 28.6 | 3.72 | 766±42.9 | 5.60 |
| | Medium | 50.8 | 49.3± 2.27 | 4.~~6~~58 | 48.3± 3.81 | 7.~~9~~89 |
| | Low | 3.05 | 3.39± 0.276 | 8.~~1~~07 | 3.43± 0.32 | 9.31 |
| *l*CK | High | 815 | 782±17.2 | 2.23 | 766± 29.1 | 3.82 |
| | Medium | 50.8 | 47.2± 2.03 | 4.34 | 47.8± 2.63 | 5.51 |
| | Low | 3.05 | 3.45± 0.187 | 5.~~1~~09 | 3.42± 0.275 | 7.~~8~~79 |
| L1 | High | 540 | 518± 15.6 | 2.91 | 502± 15.6 | 3.01 |
| | Medium | 67.2 | 65.2± 2.80 | 4.13 | 63.2± 2.91 | 4.~~9~~88 |
| | Low | 2.22 | 2.44± 0.163 | 6.42 | 2.53± 0.184 | 7.03 |
| L2 | High | 540 | 502± 17.6 | 3.32 | 518± 19.2 | 3.~~6~~58 |
| | Medium | 67.2 | 65.9± 2.70 | 3.94 | 64.2± 2.95 | 4.72 |

| | | | | | |
|---|---|---|---|---|---|
| Low | 2.22 | 2.42± 0.118 | 4.~~7~~68 | 2.51± 0.132 | 5.~~3~~29 |

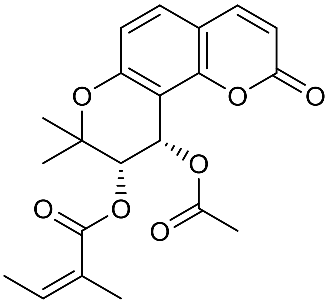

*d*PA

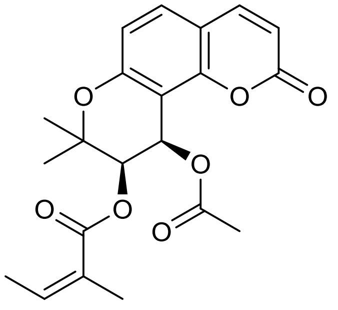

*l*PA

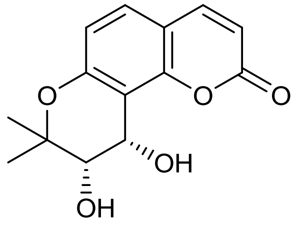

*l*CK

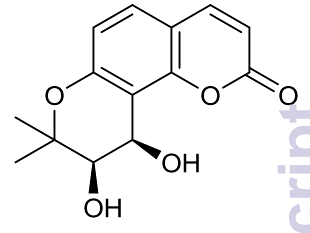

*d*CK

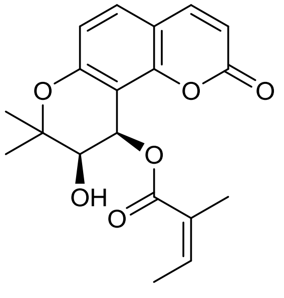

L1

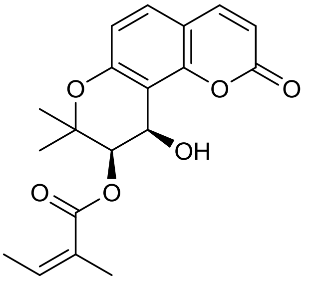

L2

Figure 1

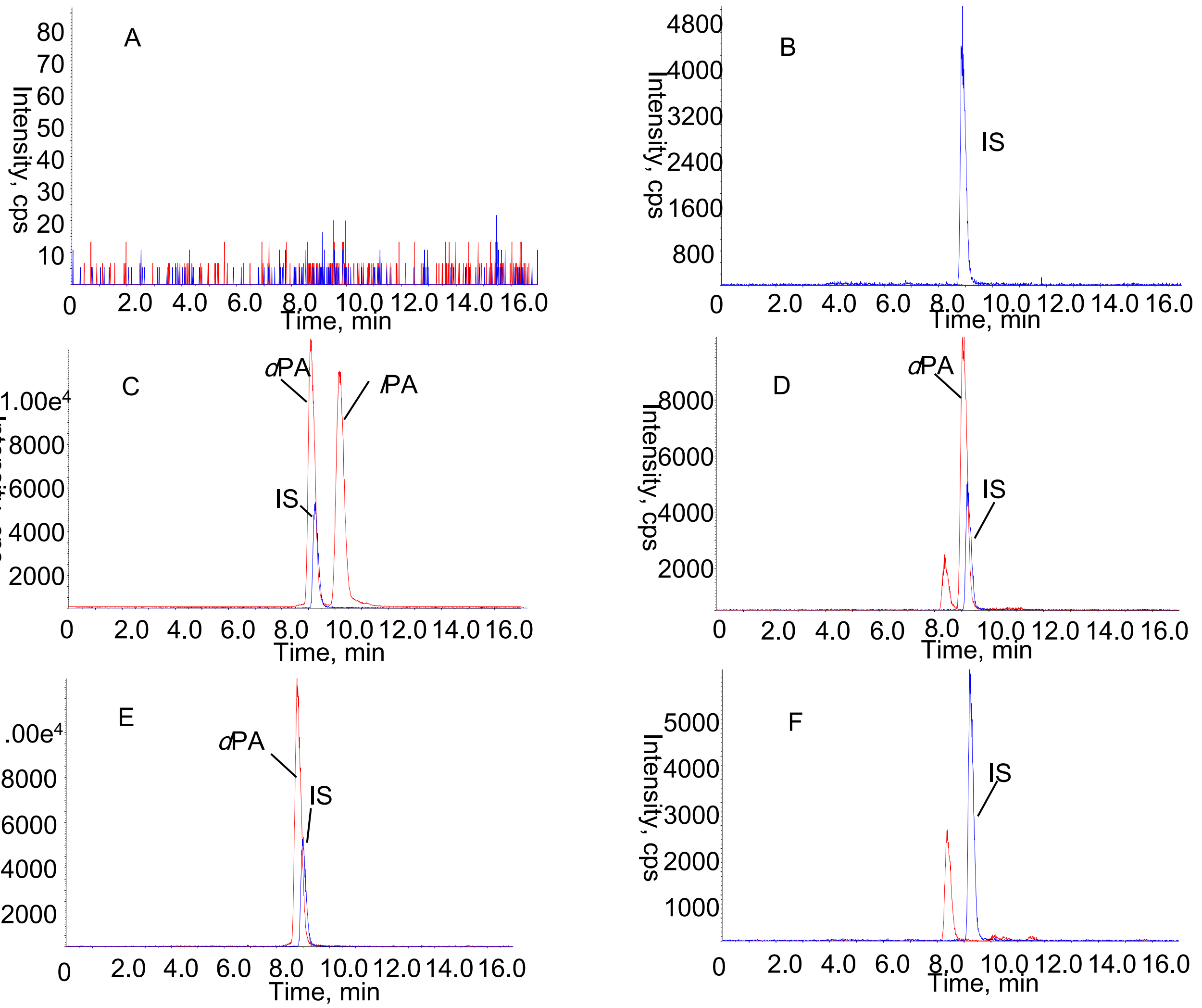
A
Intensity, cps
80
70
60
50
40
30
20
10
0
2.0
4.0
6.0
8.0
10.0
12.0
14.0
16.0
Time, min
B
IS
Intensity, cps
4800
4000
3200
2400
1600
800
C
dPA
lPA
IS
1.00e4
8000
6000
4000
2000
D
8000
6000
4000
2000
E
5000
3000
1000
F

Figure 2

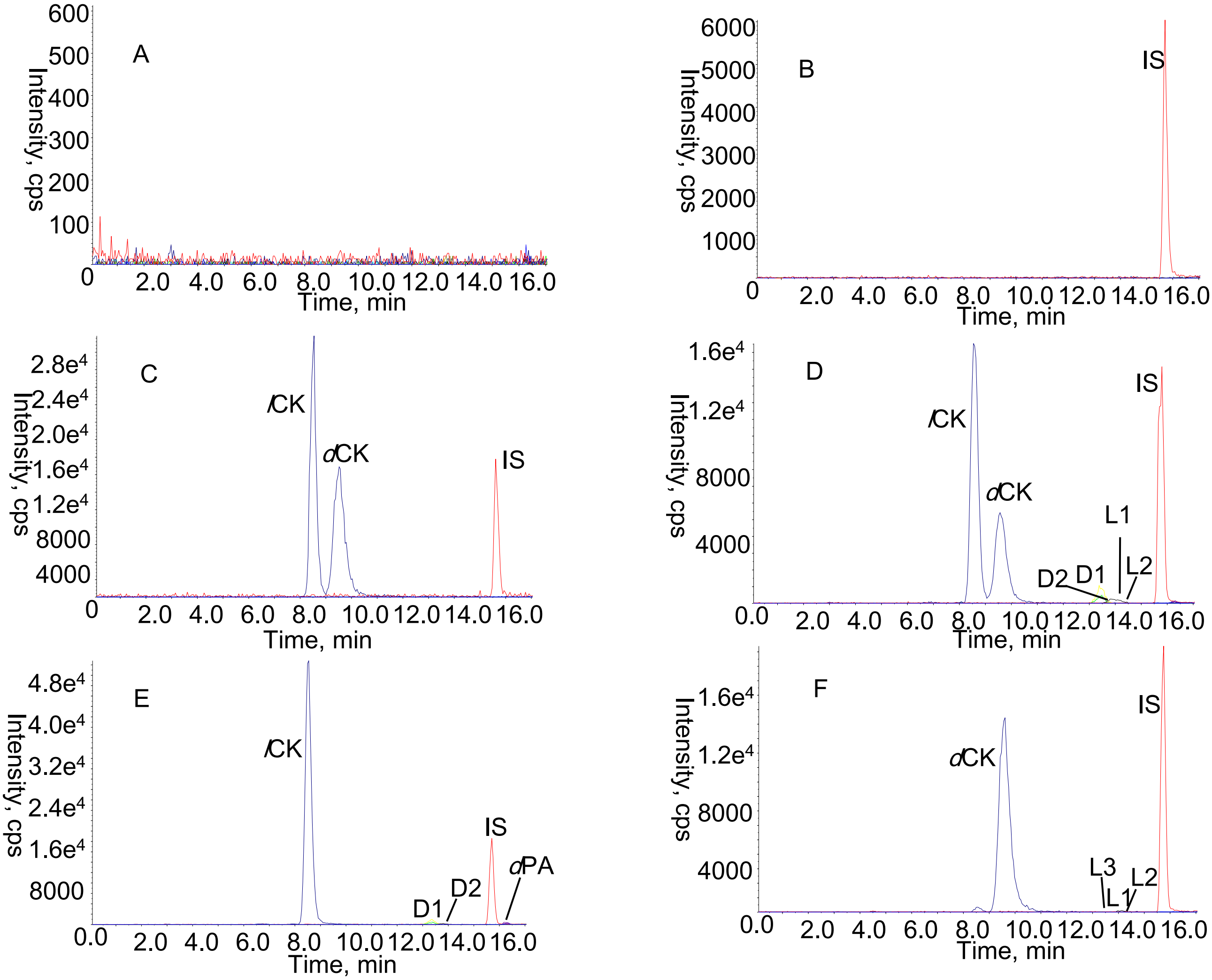
A
Intensity, cps
Time, min
B
IS
C
*l*CK
*d*CK
IS
D
*l*CK
*d*CK
L1
L2
D2
D1
IS
E
*l*CK
IS
*d*PA
D1
D2
F
*d*CK
IS
L3
L1
L2

Figure 3

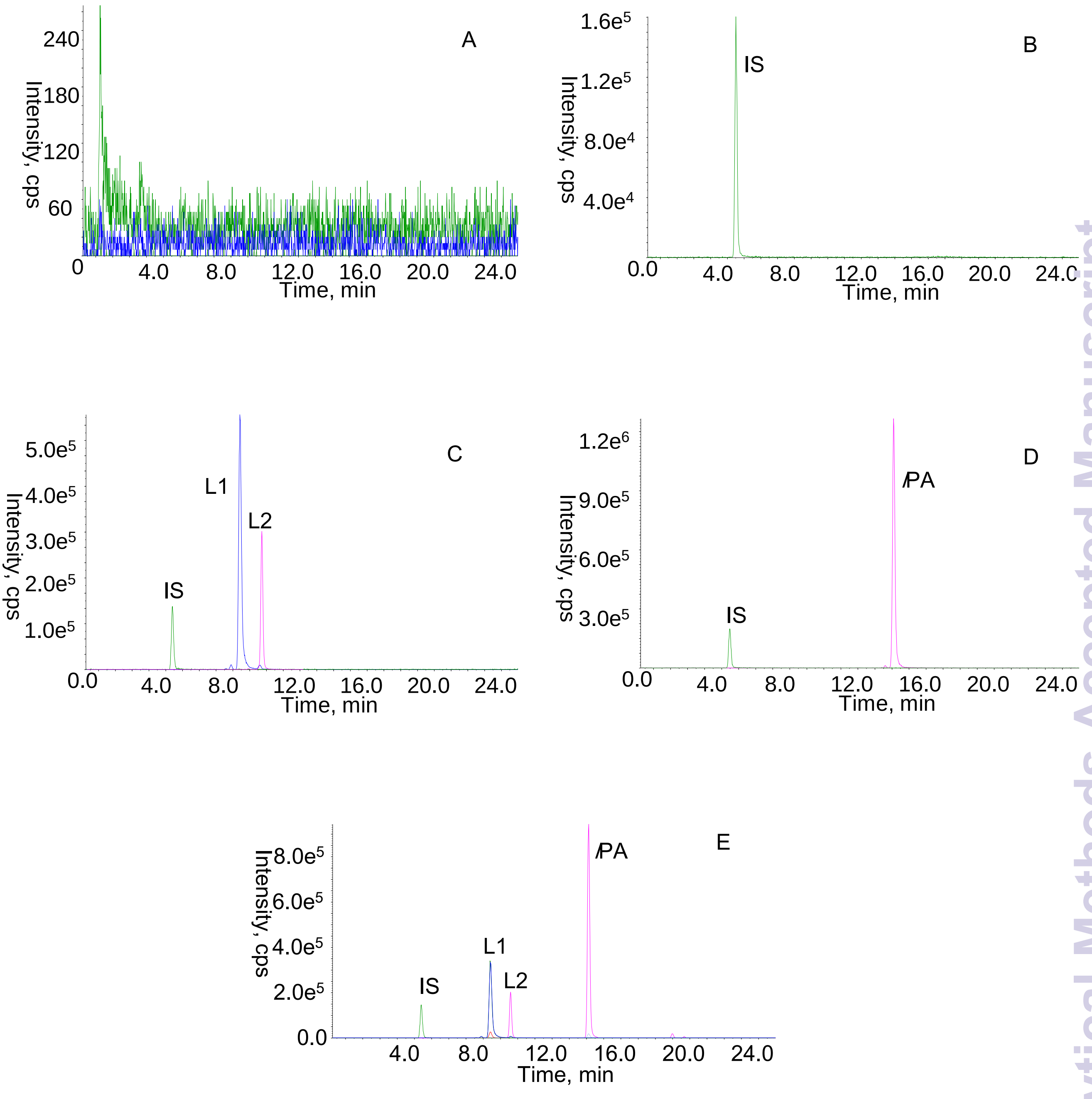
A
Intensity, cps
Time, min
B
IS
Intensity, cps
Time, min
C
L1
L2
IS
Intensity, cps
Time, min
D
PA
IS
Intensity, cps
Time, min
E
PA
L1
L2
IS
Intensity, cps
Time, min



Figure 4